

Determination of the Branching Fraction for Inclusive Decays

$$B \rightarrow X_s \gamma$$

The *BABAR* Collaboration

July 24 2002

Abstract

We present a preliminary determination of the inclusive branching fraction for the rare radiative penguin transition $B \rightarrow X_s \gamma$. The measurement is based on a data sample of 60 million $B\bar{B}$ pairs collected between 1999 and 2001 with the *BABAR* detector at the PEP-II asymmetric-energy e^+e^- B Factory at SLAC. We study events containing a high-energy photon from one B (or \bar{B}) decay and a tagging primary lepton from the decay of the other B meson. By this means, we are able to reduce a significant component of the background without introduction of model dependent uncertainties in the event selection efficiency. We determine the branching fraction $\mathcal{B}(B \rightarrow X_s \gamma) = [3.88 \pm 0.36(\text{stat.}) \pm 0.37(\text{syst.}) \pm_{0.23}^{0.43}(\text{model})] \times 10^{-4}$, which is consistent with Standard Model predictions and provides a constraint on possible new physics contributions to the electromagnetic penguin amplitude in B decays.

Contributed to the 31st International Conference on High Energy Physics,
7/24—7/31/2002, Amsterdam, The Netherlands

Stanford Linear Accelerator Center, Stanford University, Stanford, CA 94309

Work supported in part by Department of Energy contract DE-AC03-76SF00515.

The BABAR Collaboration,

B. Aubert, D. Boutigny, J.-M. Gaillard, A. Hicheur, Y. Karyotakis, J. P. Lees, P. Robbe, V. Tisserand,
A. Zghiche

Laboratoire de Physique des Particules, F-74941 Annecy-le-Vieux, France

A. Palano, A. Pompili

Università di Bari, Dipartimento di Fisica and INFN, I-70126 Bari, Italy

J. C. Chen, N. D. Qi, G. Rong, P. Wang, Y. S. Zhu

Institute of High Energy Physics, Beijing 100039, China

G. Eigen, I. Ofte, B. Stugu

University of Bergen, Inst. of Physics, N-5007 Bergen, Norway

G. S. Abrams, A. W. Borgland, A. B. Breon, D. N. Brown, J. Button-Shafer, R. N. Cahn, E. Charles,
M. S. Gill, A. V. Gritsan, Y. Groysman, R. G. Jacobsen, R. W. Kadel, J. Kadyk, L. T. Kerth,
Yu. G. Kolomensky, J. F. Kral, C. LeClerc, M. E. Levi, G. Lynch, L. M. Mir, P. J. Oddone, T. J. Orimoto,
M. Pripstein, N. A. Roe, A. Romosan, M. T. Ronan, V. G. Shelkov, A. V. Telnov, W. A. Wenzel

Lawrence Berkeley National Laboratory and University of California, Berkeley, CA 94720, USA

T. J. Harrison, C. M. Hawkes, D. J. Knowles, S. W. O'Neale, R. C. Penny, A. T. Watson, N. K. Watson

University of Birmingham, Birmingham, B15 2TT, United Kingdom

T. Deppermann, K. Goetzen, H. Koch, B. Lewandowski, K. Peters, H. Schmuecker, M. Steinke

Ruhr Universität Bochum, Institut für Experimentalphysik 1, D-44780 Bochum, Germany

N. R. Barlow, W. Bhimji, J. T. Boyd, N. Chevalier, P. J. Clark, W. N. Cottingham, C. Mackay,
F. F. Wilson

University of Bristol, Bristol BS8 1TL, United Kingdom

K. Abe, C. Hearty, T. S. Mattison, J. A. McKenna, D. Thiessen

University of British Columbia, Vancouver, BC, Canada V6T 1Z1

S. Jolly, A. K. McKemey

Brunel University, Uxbridge, Middlesex UB8 3PH, United Kingdom

V. E. Blinov, A. D. Bukin, A. R. Buzykaev, V. B. Golubev, V. N. Ivanchenko, A. A. Korol,
E. A. Kravchenko, A. P. Onuchin, S. I. Serebnyakov, Yu. I. Skovpen, A. N. Yushkov

Budker Institute of Nuclear Physics, Novosibirsk 630090, Russia

D. Best, M. Chao, D. Kirkby, A. J. Lankford, M. Mandelkern, S. McMahon, D. P. Stoker

University of California at Irvine, Irvine, CA 92697, USA

K. Arisaka, C. Buchanan, S. Chun

University of California at Los Angeles, Los Angeles, CA 90024, USA

H. K. Hadavand, E. J. Hill, D. B. MacFarlane, H. Paar, S. Prell, Sh. Rahatlou, G. Raven, U. Schwanke,
V. Sharma

University of California at San Diego, La Jolla, CA 92093, USA

J. W. Berryhill, C. Campagnari, B. Dahmes, P. A. Hart, N. Kuznetsova, S. L. Levy, O. Long, A. Lu,
M. A. Mazur, J. D. Richman, W. Verkerke

University of California at Santa Barbara, Santa Barbara, CA 93106, USA

J. Beringer, A. M. Eisner, M. Grothe, C. A. Heusch, W. S. Lockman, T. Pulliam, T. Schalk, R. E. Schmitz,
B. A. Schumm, A. Seiden, M. Turri, W. Walkowiak, D. C. Williams, M. G. Wilson

University of California at Santa Cruz, Institute for Particle Physics, Santa Cruz, CA 95064, USA

E. Chen, G. P. Dubois-Felsmann, A. Dvoretzki, D. G. Hitlin, F. C. Porter, A. Ryd, A. Samuel, S. Yang
California Institute of Technology, Pasadena, CA 91125, USA

S. Jayatileke, G. Mancinelli, B. T. Meadows, M. D. Sokoloff

University of Cincinnati, Cincinnati, OH 45221, USA

T. Barillari, P. Bloom, W. T. Ford, U. Nauenberg, A. Olivas, P. Rankin, J. Roy, J. G. Smith, W. C. van
Hoek, L. Zhang

University of Colorado, Boulder, CO 80309, USA

J. L. Harton, T. Hu, M. Krishnamurthy, A. Soffer, W. H. Toki, R. J. Wilson, J. Zhang

Colorado State University, Fort Collins, CO 80523, USA

D. Altenburg, T. Brandt, J. Brose, T. Colberg, M. Dickopp, R. S. Dubitzky, A. Hauke, E. Maly,
R. Müller-Pfefferkorn, S. Otto, K. R. Schubert, R. Schwierz, B. Spaan, L. Wilden

Technische Universität Dresden, Institut für Kern- und Teilchenphysik, D-01062 Dresden, Germany

D. Bernard, G. R. Bonneaud, F. Brochard, J. Cohen-Tanugi, S. Ferrag, S. T'Jampens, Ch. Thiebaux,
G. Vasileiadis, M. Verderi

Ecole Polytechnique, LLR, F-91128 Palaiseau, France

A. Anjomshoaa, R. Bernet, A. Khan, D. Lavin, F. Muheim, S. Playfer, J. E. Swain, J. Tinslay

University of Edinburgh, Edinburgh EH9 3JZ, United Kingdom

M. Falbo

Elon University, Elon University, NC 27244-2010, USA

C. Borean, C. Bozzi, L. Piemontese, A. Sarti

Università di Ferrara, Dipartimento di Fisica and INFN, I-44100 Ferrara, Italy

E. Treadwell

Florida A&M University, Tallahassee, FL 32307, USA

F. Anulli,¹ R. Baldini-Ferrolì, A. Calcaterra, R. de Sangro, D. Falciai, G. Finocchiaro, P. Patteri,
I. M. Peruzzi,¹ M. Piccolo, A. Zallo

Laboratori Nazionali di Frascati dell'INFN, I-00044 Frascati, Italy

S. Bagnasco, A. Buzzo, R. Contri, G. Crosetti, M. Lo Vetere, M. Macri, M. R. Monge, S. Passaggio,
F. C. Pastore, C. Patrignani, E. Robutti, A. Santroni, S. Tosi

Università di Genova, Dipartimento di Fisica and INFN, I-16146 Genova, Italy

¹ Also with Università di Perugia, I-06100 Perugia, Italy

S. Bailey, M. Morii

Harvard University, Cambridge, MA 02138, USA

R. Bartoldus, G. J. Grenier, U. Mallik

University of Iowa, Iowa City, IA 52242, USA

J. Cochran, H. B. Crawley, J. Lamsa, W. T. Meyer, E. I. Rosenberg, J. Yi

Iowa State University, Ames, IA 50011-3160, USA

M. Davier, G. Grosdidier, A. Höcker, H. M. Lacker, S. Laplace, F. Le Diberder, V. Lepeltier, A. M. Lutz,
T. C. Petersen, S. Plaszczynski, M. H. Schune, L. Tantot, S. Trincaz-Duvoid, G. Wormser

Laboratoire de l'Accélérateur Linéaire, F-91898 Orsay, France

R. M. Bionta, V. Brigljević, D. J. Lange, M. Mugge, K. van Bibber, D. M. Wright

Lawrence Livermore National Laboratory, Livermore, CA 94550, USA

A. J. Bevan, J. R. Fry, E. Gabathuler, R. Gamet, M. George, M. Kay, D. J. Payne, R. J. Sloane,
C. Touramanis

University of Liverpool, Liverpool L69 3BX, United Kingdom

M. L. Aspinwall, D. A. Bowerman, P. D. Dauncey, U. Egede, I. Eschrich, G. W. Morton, J. A. Nash,
P. Sanders, D. Smith, G. P. Taylor

University of London, Imperial College, London, SW7 2BW, United Kingdom

J. J. Back, G. Bellodi, P. Dixon, P. F. Harrison, R. J. L. Potter, H. W. Shorthouse, P. Strother, P. B. Vidal

Queen Mary, University of London, E1 4NS, United Kingdom

G. Cowan, H. U. Flaecher, S. George, M. G. Green, A. Kurup, C. E. Marker, T. R. McMahon, S. Ricciardi,
F. Salvatore, G. Vaitsas, M. A. Winter

University of London, Royal Holloway and Bedford New College, Egham, Surrey TW20 0EX, United Kingdom

D. Brown, C. L. Davis

University of Louisville, Louisville, KY 40292, USA

J. Allison, R. J. Barlow, A. C. Forti, F. Jackson, G. D. Lafferty, A. J. Lyon, N. Savvas, J. H. Weatherall,
J. C. Williams

University of Manchester, Manchester M13 9PL, United Kingdom

A. Farbin, A. Jawahery, V. Lillard, D. A. Roberts, J. R. Schieck

University of Maryland, College Park, MD 20742, USA

G. Blaylock, C. Dallapiccola, K. T. Flood, S. S. Hertzbach, R. Kofler, V. B. Koptchev, T. B. Moore,
H. Staengle, S. Willocq

University of Massachusetts, Amherst, MA 01003, USA

B. Brau, R. Cowan, G. Sciolla, F. Taylor, R. K. Yamamoto

Massachusetts Institute of Technology, Laboratory for Nuclear Science, Cambridge, MA 02139, USA

M. Milek, P. M. Patel

McGill University, Montréal, QC, Canada H3A 2T8

F. Palombo

Università di Milano, Dipartimento di Fisica and INFN, I-20133 Milano, Italy

J. M. Bauer, L. Cremaldi, V. Eschenburg, R. Kroeger, J. Reidy, D. A. Sanders, D. J. Summers
University of Mississippi, University, MS 38677, USA

C. Hast, P. Taras

Université de Montréal, Laboratoire René J. A. Lévesque, Montréal, QC, Canada H3C 3J7

H. Nicholson

Mount Holyoke College, South Hadley, MA 01075, USA

C. Cartaro, N. Cavallo, G. De Nardo, F. Fabozzi, C. Gatto, L. Lista, P. Paolucci, D. Piccolo, C. Sciacca
Università di Napoli Federico II, Dipartimento di Scienze Fisiche and INFN, I-80126, Napoli, Italy

J. M. LoSecco

University of Notre Dame, Notre Dame, IN 46556, USA

J. R. G. Alsmiller, T. A. Gabriel

Oak Ridge National Laboratory, Oak Ridge, TN 37831, USA

J. Brau, R. Frey, M. Iwasaki, C. T. Potter, N. B. Sinev, D. Strom, E. Torrence

University of Oregon, Eugene, OR 97403, USA

F. Colecchia, A. Dorigo, F. Galeazzi, M. Margoni, M. Morandin, M. Posocco, M. Rotondo, F. Simonetto,
R. Stroili, C. Voci

Università di Padova, Dipartimento di Fisica and INFN, I-35131 Padova, Italy

M. Benayoun, H. Briand, J. Chauveau, P. David, Ch. de la Vaissière, L. Del Buono, O. Hamon,
Ph. Leruste, J. Ocariz, M. Pivk, L. Roos, J. Stark

Universités Paris VI et VII, Lab de Physique Nucléaire H. E., F-75252 Paris, France

P. F. Manfredi, V. Re, V. Speziali

Università di Pavia, Dipartimento di Elettronica and INFN, I-27100 Pavia, Italy

L. Gladney, Q. H. Guo, J. Panetta

University of Pennsylvania, Philadelphia, PA 19104, USA

C. Angelini, G. Batignani, S. Bettarini, M. Bondioli, F. Bucci, G. Calderini, E. Campagna, M. Carpinelli,
F. Forti, M. A. Giorgi, A. Lusiani, G. Marchiori, F. Martinez-Vidal, M. Morganti, N. Neri, E. Paoloni,
M. Rama, G. Rizzo, F. Sandrelli, G. Triggiani, J. Walsh

Università di Pisa, Scuola Normale Superiore and INFN, I-56010 Pisa, Italy

M. Haire, D. Judd, K. Paick, L. Turnbull, D. E. Wagoner

Prairie View A&M University, Prairie View, TX 77446, USA

J. Albert, G. Cavoto,² N. Danielson, P. Elmer, C. Lu, V. Miftakov, J. Olsen, S. F. Schaffner,
A. J. S. Smith, A. Tumanov, E. W. Varnes

Princeton University, Princeton, NJ 08544, USA

² Also with Università di Roma La Sapienza, Roma, Italy

F. Bellini, D. del Re, R. Faccini,³ F. Ferrarotto, F. Ferroni, E. Leonardi, M. A. Mazzone, S. Morganti,
G. Piredda, F. Safai Tehrani, M. Serra, C. Voena

Università di Roma La Sapienza, Dipartimento di Fisica and INFN, I-00185 Roma, Italy

S. Christ, G. Wagner, R. Waldi

Universität Rostock, D-18051 Rostock, Germany

T. Adye, N. De Groot, B. Franek, N. I. Geddes, G. P. Gopal, S. M. Xella

Rutherford Appleton Laboratory, Chilton, Didcot, Oxon, OX11 0QX, United Kingdom

R. Aleksan, S. Emery, A. Gaidot, P.-F. Giraud, G. Hamel de Monchenault, W. Kozanecki, M. Langer,
G. W. London, B. Mayer, G. Schott, B. Serfass, G. Vasseur, Ch. Yeche, M. Zito

DAPNIA, Commissariat à l'Energie Atomique/Saclay, F-91191 Gif-sur-Yvette, France

M. V. Purohit, A. W. Weidemann, F. X. Yumiceva

University of South Carolina, Columbia, SC 29208, USA

I. Adam, D. Aston, N. Berger, A. M. Boyarski, M. R. Convery, D. P. Coupal, D. Dong, J. Dorfan,
W. Dunwoodie, R. C. Field, T. Glanzman, S. J. Gowdy, E. Grauges, T. Haas, T. Hadig, V. Halyo,
T. Himel, T. Hryn'ova, M. E. Huffer, W. R. Innes, C. P. Jessop, M. H. Kelsey, P. Kim, M. L. Kocian,
U. Langenegger, D. W. G. S. Leith, S. Luitz, V. Luth, H. L. Lynch, H. Marsiske, S. Menke, R. Messner,
D. R. Muller, C. P. O'Grady, V. E. Ozcan, A. Perazzo, M. Perl, S. Petrak, H. Quinn, B. N. Ratcliff,
S. H. Robertson, A. Roodman, A. A. Salnikov, T. Schietinger, R. H. Schindler, J. Schwiening, G. Simi,
A. Snyder, A. Soha, S. M. Spanier, J. Stelzer, D. Su, M. K. Sullivan, H. A. Tanaka, J. Va'vra,
S. R. Wagner, M. Weaver, A. J. R. Weinstein, W. J. Wisniewski, D. H. Wright, C. C. Young

Stanford Linear Accelerator Center, Stanford, CA 94309, USA

P. R. Burchat, C. H. Cheng, T. I. Meyer, C. Roat

Stanford University, Stanford, CA 94305-4060, USA

R. Henderson

TRIUMF, Vancouver, BC, Canada V6T 2A3

W. Bugg, H. Cohn

University of Tennessee, Knoxville, TN 37996, USA

J. M. Izen, I. Kitayama, X. C. Lou

University of Texas at Dallas, Richardson, TX 75083, USA

F. Bianchi, M. Bona, D. Gamba

Università di Torino, Dipartimento di Fisica Sperimentale and INFN, I-10125 Torino, Italy

L. Bosisio, G. Della Ricca, S. Dittongo, L. Lanceri, P. Poropat, L. Vitale, G. Vuagnin

Università di Trieste, Dipartimento di Fisica and INFN, I-34127 Trieste, Italy

R. S. Panvini

Vanderbilt University, Nashville, TN 37235, USA

³ Also with University of California at San Diego, La Jolla, CA 92093, USA

S. W. Banerjee, C. M. Brown, D. Fortin, P. D. Jackson, R. Kowalewski, J. M. Roney

University of Victoria, Victoria, BC, Canada V8W 3P6

H. R. Band, S. Dasu, M. Datta, A. M. Eichenbaum, H. Hu, J. R. Johnson, R. Liu, F. Di Lodovico,
A. Mohapatra, Y. Pan, R. Prepost, I. J. Scott, S. J. Sekula, J. H. von Wimmersperg-Toeller, J. Wu,
S. L. Wu, Z. Yu

University of Wisconsin, Madison, WI 53706, USA

H. Neal

Yale University, New Haven, CT 06511, USA

1 Introduction

The parton-level $b \rightarrow s\gamma$ “radiative penguin” transition rate can be calculated at next-to-leading order to a precision of 10% in the Standard Model (SM) [1]. The presence of non-SM particles in the virtual loop mediating this transition may lead to substantial deviations from this predicted rate and has been the subject of numerous theoretical investigations [2]. The inclusive $B \rightarrow X_s\gamma$ rate is equal to the calculated parton-level $b \rightarrow s\gamma$ rate according to quark-hadron duality [1]. There have been several measurements of the branching fraction for $B \rightarrow X_s\gamma$ to date [3]. The confinement of the b quark in the B meson results in model dependent assumptions for the E_γ spectrum, while the X_s system fragments non-perturbatively into the detectable final state particles. Thus, in order to access the parton model process, it is desirable to impose as few requirements as possible on the $X_s\gamma$ system, motivating a fully-inclusive approach. This, however, makes the measurement susceptible to large backgrounds, which must be suppressed without making such requirements.

In this paper we present a measurement of the branching fraction $\mathcal{B}(B \rightarrow X_s\gamma)$ in which a significant component of the background is removed by making requirements on the other B meson in the event, rather than on the signal $B \rightarrow X_s\gamma$ decay. The remaining background is constrained by independent control samples. Although a requirement on E_γ is still necessary, the accessible energy range is limited by the statistics of the control samples, which scale directly with the signal size. Hence this technique scales well with the increasing data sample anticipated at *BABAR*. This fully-inclusive technique does not distinguish between decays of charged and neutral B mesons, so both are used. For simplicity we refer to both B and \bar{B} as “ B mesons”.

2 The *BABAR* detector and dataset

The data were collected with the *BABAR* detector at the PEP-II asymmetric-energy $e^+(3.1 \text{ GeV}) - e^-(9 \text{ GeV})$ storage ring. A description of the *BABAR* detector can be found in Ref. [4]. Charged particles are detected and their momenta measured by a combination of a silicon vertex tracker (SVT), consisting of five double-sided layers, and a central drift chamber (DCH), in a 1.5-T solenoidal field. We identify leptons and hadrons with measurements from all detector systems, including the energy loss (dE/dx) in the DCH and SVT. Electrons and photons are identified by a CsI electromagnetic calorimeter (EMC). Muons are identified in the instrumented flux return (IFR). A Cherenkov ring imaging detector (DIRC) covering the central region provides particle identification.

We use Monte Carlo simulations of the *BABAR* detector based on GEANT 4.0 [5] to optimize our selection criteria, to determine signal efficiencies and to estimate part of the background component. Events taken from random triggers are mixed with simulated events to take beam backgrounds and some varying detector conditions into account.

The results in this paper are based upon an integrated luminosity of $54.6 \pm 0.8 \text{ fb}^{-1}$ of data, corresponding to $(59.6 \pm 0.7) \times 10^6 B\bar{B}$ meson pairs recorded at the $\mathcal{T}(4S)$ resonance (“on-resonance”) and $6.40 \pm 0.10 \text{ fb}^{-1}$ at 40 MeV below this energy (“off-resonance”). The off-resonance data, which constitute a fraction $f_{\text{off}} = 10.5\%$ of the total data set, are used for background estimation. The number of $B\bar{B}$ meson pairs is determined from the excess hadronic events relative to muon pairs in on-resonance data compared to off-resonance data [4].

3 Analysis method

The $B \rightarrow X_s \gamma$ decay signature is characterized by the high energy photon. The background to the $B \rightarrow X_s \gamma$ signal consists of two components. First, it can arise from other B meson decays, in which the photon candidates are predominantly from π^0 or η (or rarely ω) decays, or – in a small fraction of cases – from a hadronic interaction of a neutron or K_L^0 in the electromagnetic calorimeter. Second, it can arise from continuum $q\bar{q}$ or $\tau^+\tau^-$ production, where q can be a u, d, s or c quark, with the high-energy photon originating either from initial-state radiation (ISR) or from similar sources to those in B decays. Figure 1 demonstrates the scale of the background rejection problem (based on Monte Carlo simulation).

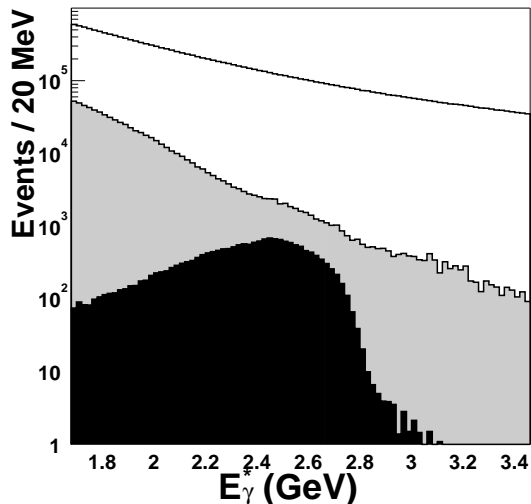


Figure 1: The energy distribution, in the $\Upsilon(4S)$ center of mass, of simulated photon candidates, after “photon quality” cuts designed to reduce backgrounds from π^0 s, η s and hadrons, but before other selection requirements. Shown are $B \rightarrow X_s \gamma$ signal (dark shading), $B\bar{B}$ background (grey shading) and continuum background (unshaded), all normalized to 54.6 fb^{-1} . The high-end tail for $B\bar{B}$ is mainly due to residual hadrons.

The method for extracting the signal from data is to subtract the continuum background based on off-resonance data, and the $B\bar{B}$ contribution based on Monte Carlo predictions, where the latter are validated (and if necessary corrected) using our control samples. A series of selection requirements is made to greatly suppress backgrounds (primarily continuum) before the subtraction. The selection criteria for this analysis are optimized for statistical precision by maximizing $n_S^2 / (n_S + n_B + n_C / f_{\text{off}})$. The number of signal candidates n_S is estimated using a Monte Carlo simulation that incorporates the model of Kagan and Neubert [1] for the E_γ spectrum and assumes a central theoretical value of $\mathcal{B}(B \rightarrow X_s \gamma) = 3.45 \times 10^{-4}$ [1]. The $B\bar{B}$ and continuum backgrounds, n_B and n_C , are estimated with Monte Carlo simulation. The signal and background expectations are normalized to 54.6 fb^{-1} . The continuum is additionally weighted by $1/f_{\text{off}}$ in the optimization to allow for the smaller size of the off-resonance data set.

Initially we require a high-energy photon candidate with $1.5 < E_\gamma^* < 3.5 \text{ GeV}$ in the e^+e^- center-of-mass frame. (An asterisk denotes quantities computed in the e^+e^- center-of-mass frame,

as opposed to the laboratory frame.) This is a loose selection that is tightened later to define the signal region and also control “sideband” regions. A photon candidate is defined as a localized energy maximum [4] in the calorimeter acceptance $-0.74 < \cos \theta < 0.93$, where θ is the lab-frame polar angle relative to the e^- beam direction. It must be isolated by 40 cm at the inner surface of the EMC from any other photon candidate or track. We veto candidates whose lateral energy profile is inconsistent with a single photon shower; these can arise from hadronic interactions in the calorimeter, or from π^0 s in which the decay photons have merged into one shower (“merged π^0 s”). In addition we veto photons from a $\pi^0(\eta)$ when the invariant mass of the combination with any other photon of energy greater than 50(250) MeV is within $\approx 2.7(2.2)$ sigma of the nominal $\pi^0(\eta)$ mass, $115(508) < M_{\gamma\gamma} < 155(588)$ MeV/ c^2 . However, we retain such vetoed photons as a control sample to validate the Monte Carlo modeling of the $B\bar{B}$ background. The photon candidates that fail the lateral profile cut form the “hadron anti-veto” sample (it also includes a small component of merged π^0 s); while the photons that pass the lateral profile cut, but are rejected by the π^0 or η veto, form the “ $\pi^0(\eta)$ anti-veto sample”. All three independent samples, the signal and the two anti-veto samples, are required to pass all the subsequent selection criteria.

To suppress continuum backgrounds we require a “lepton tag”. This is a high-momentum electron ($p_e^* > 1.3$ GeV/ c) or muon ($p_\mu^* > 1.55$ GeV/ c). For $B \rightarrow X_s \gamma$ signal events the lepton arises from the semileptonic decay of the other B meson. Leptons also occur in the continuum background, most notably from the semi-leptonic decays of charm hadrons, but are produced significantly less frequently and with lower momentum than from a B decay. An electron candidate must have a ratio of calorimeter energy to track momentum, an EMC cluster shape, a DCH dE/dx and a DIRC Cherenkov angle (if available) consistent with an electron. A muon candidate must satisfy requirements on the measured and expected number of interaction lengths penetrated, the position match between the extrapolated DCH track and IFR hits, and the average and spread of the number of IFR hits per layer. The lepton candidates that do arise from continuum events are often pions misidentified as muons or, less frequently, electrons. Fake leptons are usually not associated with an undetected neutrino, unlike real leptons from a semi-leptonic B decay. We therefore require that the missing energy in the event be greater than 1.2 GeV. Further discrimination is obtained by considering the angle between the lepton and the high-energy photon. For signal events, the cosine of this angle, $\cos \theta_{\gamma e}^*$ ($\cos \theta_{\gamma \mu}^*$), has an approximately flat distribution, except for a small peak at $\cos \theta_{\gamma \mu}^* = -1$ arising from cases where the muon candidate and photon both originate from the signal B decay. (This can occur when a pion from the X_s decay fakes a muon.) In contrast, the continuum background is strongly peaked at $\cos \theta_{\gamma e}^*$ ($\cos \theta_{\gamma \mu}^*$) = -1 as a consequence of the jet-like topology, with the peak at $\cos \theta_{\gamma e}^*$ ($\cos \theta_{\gamma \mu}^*$) = $+1$ suppressed by the photon isolation requirement. We require $\cos \theta_{\gamma e}^*$ ($\cos \theta_{\gamma \mu}^*$) > -0.75 (-0.70). This also gives a small suppression of the $B\bar{B}$ background for cases where the high energy photon and lepton arise from the same B decay. Note that, since the tagging requirement is imposed on the “other” B rather than on the signal B , we are able to reject continuum background without imposing requirements on the signal decay. The signal efficiency of the combined lepton tag, missing energy and $\cos \theta_{\gamma e}^*$ ($\cos \theta_{\gamma \mu}^*$) requirements is 5%, while the continuum background is suppressed by a factor of approximately 1200. The momentum-dependent electron and muon efficiencies used for these and other Monte Carlo results have been measured in data with a sample of radiative Bhabha events and samples of $e^+e^- \rightarrow \mu^+\mu^-\gamma$ and $e^+e^- \rightarrow e^+e^-\mu^+\mu^-$ events, respectively.

Further continuum rejection is gained by imposing selection criteria on the event topology. In the center-of-mass system $B\bar{B}$ decays are isotropic, while the inclusive $\pi^0(\eta)$ and ISR components of the continuum background have a two and three-jet topology, respectively. We compute the

ratio of the second to the zeroth order Fox-Wolfram moment [6] in both the center-of-mass frame, R_2^* , and the rest frame of the system recoiling against the high energy photon, R_2' . The recoil frame recovers the two-jet topology for ISR events. We require $R_2^* < 0.45$ and $R_2'/R_2^* < 1$. We compute the energy sums of all particles (except the photon candidate) whose momentum vectors lie within $0^\circ - 30^\circ$ and $140^\circ - 180^\circ$ cones about the photon direction, referred to as E_f^* and E_b^* , respectively. We require $E_f^* < 1.1$ GeV and $1.6 < E_b^* < 3.6$ GeV.

Figure 2 shows the Monte Carlo prediction for the E_γ^* distribution for signal, $B\bar{B}$ background and continuum background after the preceding selection criteria, and the expected E_γ^* signal distribution for different model parameters. The signal region is defined to be $2.1 < E_\gamma^* < 2.7$ GeV, while the regions $1.7 < E_\gamma^* < 1.9$ and $2.9 < E_\gamma^* < 3.5$ GeV, which are dominated by $B\bar{B}$ and continuum background, respectively, serve as “control” regions for the estimation of these background components. The choice of the final E_γ^* signal region, in particular the lower bound on E_γ^* , is a balance between the systematic uncertainty of the estimated $B\bar{B}$ component, which is the dominant systematic uncertainty of the measurement, and the model dependence. As the lower E_γ^* bound is reduced, the model dependence decreases but the $B\bar{B}$ background, which is estimated with a Monte Carlo simulation, rises sharply.

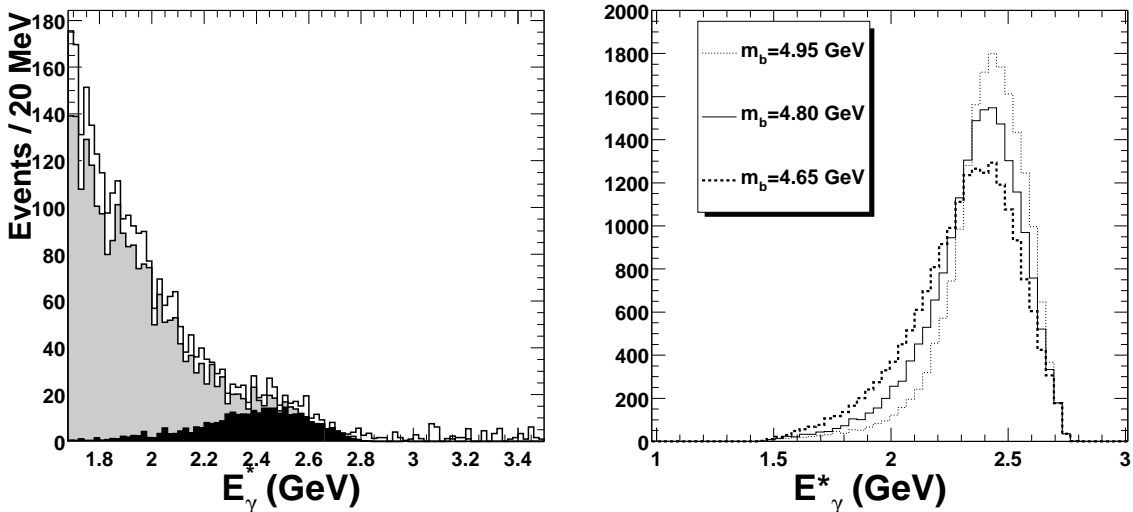


Figure 2: Left: The reconstructed E_γ^* distribution expected from Monte Carlo simulation after the selection criteria. The $B \rightarrow X_s \gamma$ signal assuming $\mathcal{B}(B \rightarrow X_s \gamma) = 3.45 \times 10^{-4}$ (dark shading), $B\bar{B}$ background (grey shading) and continuum background (unshaded) are normalized to 54.6 fb^{-1} . Right: The generated E_γ^* spectrum before cuts (arbitrary normalization) for different values of the b quark mass m_b , using the model of Kagan and Neubert [1]. Our signal region is defined for the corresponding reconstructed quantity as $2.1 < E_\gamma^* < 2.7$ GeV.

4 Systematic studies

In Table 1 we list the fractional systematic uncertainties on the extracted branching fraction $\mathcal{B}(B \rightarrow X_s \gamma)$. The dominant uncertainty is the modeling of the $B\bar{B}$ background. To test the modeling of the E_γ^* spectrum of the $B\bar{B}$ background component, we compare the two anti-veto samples, after

Table 1: The systematic error expressed as a percentage of $\mathcal{B}(B \rightarrow X_s \gamma)$. The total is the quadratic sum of all contributions.

Systematic Uncertainty	$\Delta\mathcal{B}(B \rightarrow X_s \gamma)/\mathcal{B}(\%)$
$B\bar{B}$ background estimation	± 7.8
Signal Monte Carlo statistics	± 2.6
Photon efficiency	± 2.5
Lepton tag efficiency	± 2.0
Energy scale	± 1.0
Energy resolution	± 1.0
Photon distance requirement	± 2.0
π^0/η veto	± 1.0
$B\bar{B}$ count	± 1.1
Total	± 9.3
Signal model dependence	+11.2, -5.9

the continuum contribution has been subtracted using the off-resonance data, with generic $B\bar{B}$ Monte Carlo event samples that have passed the same selection criteria described above. Figure 3 shows the comparison between Monte Carlo simulated events and data for the “ π^0 and η anti-veto sample” and the “hadron anti-veto” sample. To take any differences into account, we separately fit the ratio of the measured data to Monte Carlo prediction for each control sample with a first-order polynomial, and compute the average of the fit over the range $2.1 < E_\gamma^* < 2.7$ GeV, weighted by the E_γ^* spectrum expected for the corresponding background to our signal sample. We then correct the E_γ^* spectrum of the $B\bar{B}$ Monte Carlo simulation used to estimate the background in the signal region according to these fit results, further weighted by the relative contributions of the π^0 and η (91%) and hadronic and merged π^0 components (9%) to the background. To estimate the uncertainty in this correction we find the variation incurred when using a zero-order polynomial fit rather than first-order, or moving the lower bound of the fit region from 1.7 to 1.8 GeV, or simply considering the ratio of data to Monte Carlo events in the region $2.1 < E_\gamma^* < 2.7$ GeV. This variation is summed in quadrature to the statistical error of the first-order polynomial fit. The correction factor for the total $B\bar{B}$ background in the region $2.1 < E_\gamma^* < 2.7$ GeV is 0.89 ± 0.16 . The final uncertainty on the $B\bar{B}$ background estimate is computed by counting the expected number of Monte Carlo events and then correcting as described, with the uncertainty being the sum in quadrature of the statistical error of the Monte Carlo expectation and the uncertainty in the correction factor. This results in a corrected expectation for $B\bar{B}$ events in $2.1 < E_\gamma^* < 2.7$ GeV of 222 ± 43 . (This is translated to the fractional entry in Table 1 by dividing the uncertainty by the extracted signal from Section 5.)

The remaining systematic uncertainties are from the uncertainty in the signal efficiency due to the photon selection and the lepton tag requirements, plus a small contribution from $B\bar{B}$ event counting. The photon efficiency is measured by comparing the ratio of events $N(\tau^\pm \rightarrow h^\pm \pi^0)/N(\tau^\pm \rightarrow h^\pm \pi^0 \pi^0)$ to the previously measured branching fractions [7]. The photon isolation and π^0/η veto efficiency are dependent on the event multiplicity. Their simulation is tested by

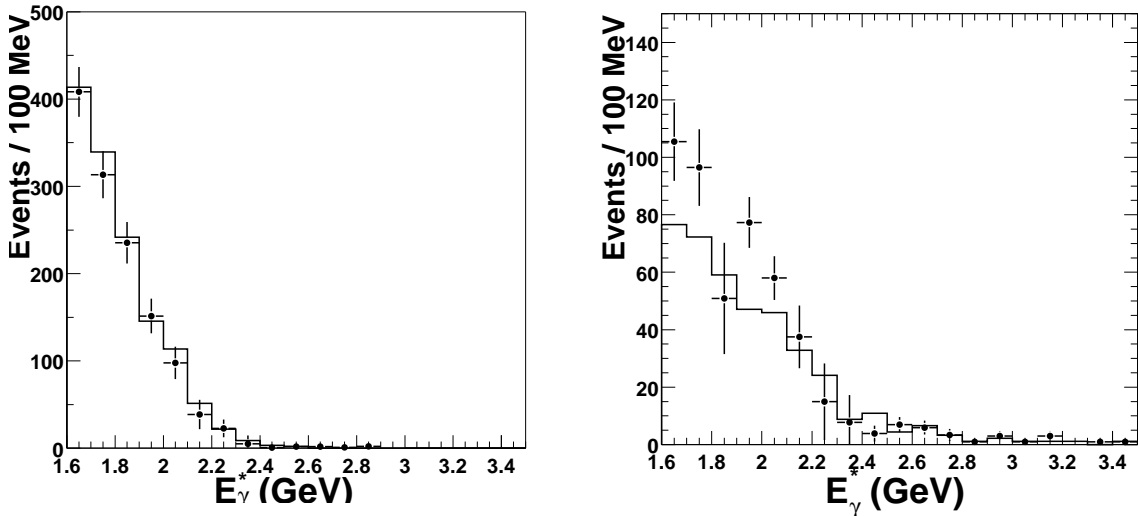


Figure 3: Left: The E_γ^* distribution for the π^0 and η anti-veto control sample for data (points) compared to the Monte Carlo prediction (solid line). Right: Corresponding distribution for the hadron anti-veto control sample.

“embedding” Monte Carlo-generated photons into both an exclusively reconstructed B meson data sample and a generic B meson Monte Carlo sample. The photon-energy resolution is measured in data using π^0 and η meson decays and a sample of virtual Compton scattering events. The energy scale uncertainty is estimated with a sample of η meson decays with approximately equal-energy photons; the deviation in the reconstructed η mass from the nominal η mass provides an estimate of the uncertainty in the measured single photon energy. Lepton tag systematics have been estimated by coherently varying the measured efficiencies by $\pm 1\sigma$. The total systematic uncertainty of 9.3% is the quadratic sum of all the contributions itemized in Table 1.

We use an E_γ^* spectrum based on the model of Kagan and Neubert [1] to determine the signal efficiency. In this model, the E_γ spectrum, which is dual to the mass spectrum of the X_s system through the relation $E_\gamma = \frac{m_B^2 - m_{X_s}^2}{2m_B}$, where E_γ is the energy of the photon in the B meson rest frame, has two components. The region $m_{X_s} < m_{\text{cutoff}}$ is described by a relativistic Breit-Wigner for the $B \rightarrow K^*(892)\gamma$ decay. The region $m_{X_s} > m_{\text{cutoff}}$ is described by a spectrum parameterized in terms of the b -quark mass m_b . The efficiency is sensitive to the value of m_b because that determines how much of the spectrum falls outside $2.1 < E_\gamma^* < 2.7$ GeV (right plot in Figure 2), but insensitive to the fraction of $K^*(892)$ or to the m_{cutoff} value. Kagan and Neubert [1] recommend varying m_b from 4.65 to 4.95 GeV/ c^2 to estimate model dependent variations. We therefore compute the efficiency of the signal using $m_b = 4.80 \pm 0.15$ GeV/ c^2 . We fix m_{cutoff} to 1.1 GeV/ c^2 , the value measured in a BABAR semi-inclusive analysis of $B \rightarrow X_s\gamma$ [8], and set the $K^*(892)$ fraction equal to the integral of the discarded continuum spectrum below m_{cutoff} for each m_b , a procedure suggested by Kagan and Neubert, to find resulting shifts of +11.2% and -5.9% in $\mathcal{B}(B \rightarrow X_s\gamma)$. To test the insensitivity of the result to the details of the relative contributions of $B \rightarrow K^*(892)\gamma$ and X_s assumed in the model, we explicitly vary m_{cutoff} by ± 100 MeV/ c^2 , and independently the fraction of $B \rightarrow K^*(892)\gamma$ by a factor of two. We find negligible additional uncertainty on $\mathcal{B}(B \rightarrow X_s\gamma)$.

5 Results

In order to reduce experimenter bias, the region $1.9 < E_\gamma^* < 2.9$ GeV was kept hidden until all selection criteria had been finalized and backgrounds estimated. Figure 4 shows the E_γ^* spectrum for data compared to the total predicted background. The control regions $1.7 < E_\gamma^* < 1.9$ GeV and $2.9 < E_\gamma^* < 3.5$ GeV show no statistically significant excess of data, as expected, but a signal is plainly visible in between. In the signal region, $2.1 < E_\gamma^* < 2.7$ GeV, we find 543 net signal events. Note that the selection procedure does not discriminate against the expected small component of $b \rightarrow d\gamma$, so these events are included in our total. Combined with a selection efficiency *within* the E_γ^* range of $1.28 \pm 0.06\%$ and the dataset size of $(59.6 \pm 0.7) \times 10^6 B\bar{B}$ meson pairs, this yield corresponds to a measurement of the partial branching fraction for $2.1 < E_\gamma^* < 2.7$ GeV of $\mathcal{B}(B \rightarrow X\gamma) = [3.55 \pm 0.32(stat.) \pm 0.32(syst.)] \times 10^{-4}$. For a Kagan and Neubert-based model with $m_b = 4.80$ GeV/ c^2 (see Fig. 2), the overall efficiency (including the effect of the E_γ^* cuts) is $1.127 \pm 0.055\%$, resulting in $\mathcal{B}(B \rightarrow X\gamma) = [4.05 \pm 0.37(stat.) \pm 0.38(syst.) \pm_{0.24}^{0.45}(model)] \times 10^{-4}$. Finally, we subtract from this a contribution from $b \rightarrow d\gamma$. In the Standard Model the theoretical expectation is $\mathcal{B}(B \rightarrow X_d\gamma)/\mathcal{B}(B \rightarrow X_s\gamma) = |V_{td}/V_{ts}|^2$. Assuming the signal efficiency for $B \rightarrow X_d\gamma$ to be equal to that for $B \rightarrow X_s\gamma$ and $|V_{td}/V_{ts}| = 0.20 \pm 0.04$ [7] we then scale the measured branching fraction by 0.96 ± 0.02 to give the preliminary result:

$$\mathcal{B}(B \rightarrow X_s\gamma) = [3.88 \pm 0.36(stat.) \pm 0.37(syst.) \pm_{0.23}^{0.43}(model)] \times 10^{-4}.$$

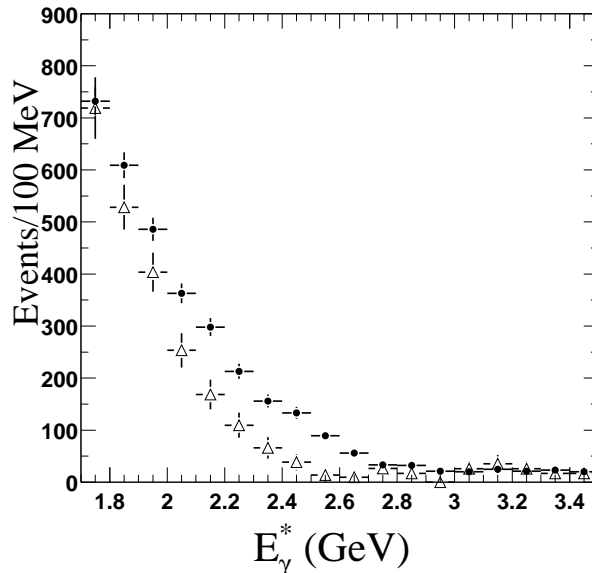


Figure 4: The E_γ^* distribution of on-resonance data (solid points) compared to background expectation. All errors are statistical only (including, just for this figure, $B\bar{B}$ background statistics). Bin-by-bin systematic uncertainties and correlations have not yet been studied; the systematics quoted in the text apply *only* to an integral measurement from 2.1 to 2.7 GeV.

6 Summary

We find a preliminary branching fraction for $B \rightarrow X_s \gamma$ of $[3.88 \pm 0.36(stat.) \pm 0.37(syst.) \pm_{0.23}^{0.43}(model)] \times 10^{-4}$ using an inclusive technique. Figure 5 compares this result with theoretical predictions and with previous measurements. We do not see any evidence for a departure from the next-to-leading order Standard Model predictions. The systematic precision is limited by the size of the $B\bar{B}$ background control samples, which scale in proportion to the signal sample. The systematic precision in turn limits the lower bound, $E_\gamma^* > 2.1$ GeV, of the signal region. As the larger datasets anticipated at the B -factory become available, the systematic uncertainty in the $B\bar{B}$ background will be reduced along with statistical uncertainties. Furthermore, this reduction in the systematic uncertainty may allow using a lower minimum- E_γ^* bound for the signal region, which will in turn lead to smaller model dependence.

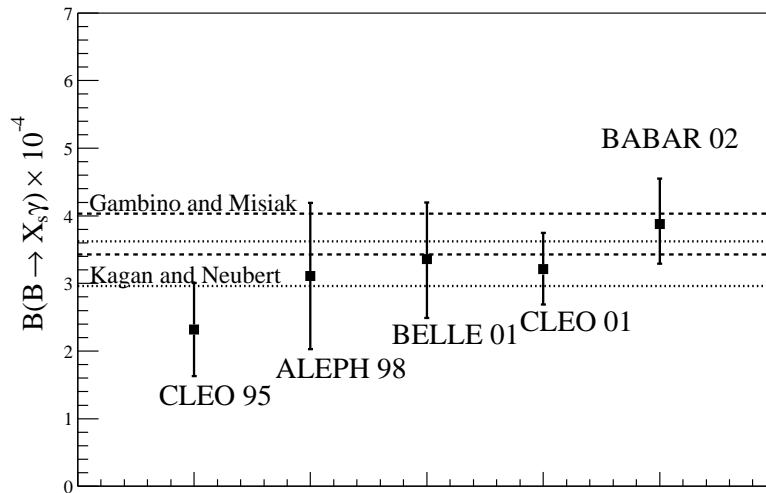


Figure 5: The *BABAR* measurement compared to previous experiments [3] and to theoretical predictions [1].

7 Acknowledgments

We are grateful for the extraordinary contributions of our PEP-II colleagues in achieving the excellent luminosity and machine conditions that have made this work possible. The success of this project also relies critically on the expertise and dedication of the computing organizations that support *BABAR*. The collaborating institutions wish to thank SLAC for its support and the kind hospitality extended to them. This work is supported by the US Department of Energy and National Science Foundation, the Natural Sciences and Engineering Research Council (Canada), Institute of High Energy Physics (China), the Commissariat à l’Energie Atomique and Institut National de Physique Nucléaire et de Physique des Particules (France), the Bundesministerium für Bildung und Forschung (Germany), the Istituto Nazionale di Fisica Nucleare (Italy), the Research Council of Norway, the Ministry of Science and Technology of the Russian Federation, and the Particle

Physics and Astronomy Research Council (United Kingdom). Individuals have received support from the A. P. Sloan Foundation, the Research Corporation, and the Alexander von Humboldt Foundation.

References

- [1] K. Abel and Y. P. Yao, Phys. Rev. D **49**, 4945 (1994); A. Ali and C. Greub, Phys. Lett. B **361**, 146 (1995); C. Greub and T. Hurth, Phys. Lett. B **380**, 2934 (1997); C. Greub, T. Hurth and D. Wyler, Phys. Lett. B **361**, 385 (1996); K. Chetyrkin, M. Misiak and M. Munz, Phys. Lett. B **400**, 296 (1997); A. J. Buras, A. Kwiatkowski and N. Pott, Phys. Lett. B **414**, 157 (1997); A. Kagan and M. Neubert, Euro. Phys. Jour **7**, 5 (1999); P. Gambino and M. Misiak, Nucl. Phys. B **611**, 338 (2001).
- [2] SPIRES lists over 500 papers. For example, see J. Hewett and J. Wells, Phys. Rev. D **55**, 5549 (1997).
- [3] CLEO Collaboration, M.S. Alam *et al.*, Phys. Rev. Lett. **74**, 2885 (1995); ALEPH Collaboration, R. Barate *et al.*, Phys. Lett. B **429**, 169 (1998); BELLE Collaboration, K. Abe *et al.*, Phys. Lett. B **511**, 151 (2001); CLEO Collaboration, S. Chen *et al.*, Phys. Rev. Lett. **87**, 251807 (2001).
- [4] The BABAR Collaboration, B. Aubert *et al.*, Nucl. Instrum. Methods **A479**, 1 (2002).
- [5] “GEANT Detector Description and Simulation Tool”, CERN Program Library Long Writeup W5013 (1994).
- [6] G. Fox and S. Wolfram, Phys. Rev. Lett. **41**, 1581 (1978).
- [7] Particle Data Group, K. Hagiwara *et al.*, Phys. Rev. D **66**, 010001 (2002).
- [8] BABAR Collaboration, B. Aubert *et al.*, submitted to this conference, BABAR-CONF-02/025, SLAC-PUB-9308 (2002).
- [9] BABAR Collaboration, B. Aubert *et al.*, Phys. Rev. Lett. **88**, 101805 (2002).